DOI: 10.1002/ejic.200900610

Molecular Interaction between a Gadolinium–Polyoxometalate and Human Serum Albumin

Li Zheng,[a,b] Ying Ma,[a] Guangjin Zhang,*[c] Jiannian Yao,*[a] Bassem S. Bassil,[d] Ulrich Kortz,[d] Bineta Keita,*[e] Pedro de Oliveira,[e] Louis Nadjo,[e] Constantin T. Craescu,[f] and Simona Miron[f]

Keywords: Gadolinium / Polyoxometalates / Fluorescence / Energy transfer / Protein structures

Polyoxometalates (POMs) show promising antibacterial, antiviral (particularly anti-HIV), antitumor, and anticancer activities, but the mechanism of these potential therapeutic effects remains to be elucidated at the molecular level. The interaction between the Gd-containing tungstosilicate $[Gd(\beta_2\text{-}SiW_{11}O_{39})_2]^{13-}$ and human serum albumin (HSA) was studied by several techniques. Fluorescence spectroscopy showed an energy transfer between the single tryptophan residue of HSA and the POM. Circular dichroism led to the conclusion that the POM significantly altered the secondary structure of HSA. Isothermal titration calorimetry revealed an enthalpy-driven binding reaction between HSA and the POM, resulting in the formation of a 1:1 complex.

Introduction

Polyoxometalates (POMs) are water-soluble, early transition-metal–oxygen anionic clusters.[1,2] They have been reported to display promising antibacterial, antiviral (particularly anti-HIV), antitumor, and anticancer activities, which may open the way towards new, innovative, and cheap therapeutic strategies for various human diseases.[1–3] Research on drug–protein interactions is important due to the prospective unraveling of drug action mechanisms and the possibility of designing novel medicines. In our previous papers,[4–6] the interactions between human serum albumin (HSA) and three types of POMs differing in their structures were studied: a Keggin, a wheel-shaped, and several Wells–Dawson POMs. The results showed that selected POMs can effectively bind the protein mainly by electrostatic interactions. It was found that the three kinds of different POM structures led to totally different binding behaviors, as far as the thermodynamics and the kinetics are concerned.[4–6] The enhancement in the luminescence of europium in a POM upon interaction with bovine serum albumin was also recently described.[7] In comparison to these normal POMs, it is anticipated that biofunctional heavy-metal-substituted POMs will show higher interest in these studies.

Gadolinium chelators are most frequently used as magnetic resonance imaging (MRI) contrast agents because of their high magnetic moment, asymmetric electronic ground state, and potential for increased MRI intensity. To date, the most commonly used MRI contrast agent in diagnostic imaging is Gd–DTPA (diethylene triamine pentaacetic acid), or related derivatives such as Gd–DTPA–BMA (bismethylamide). In comparison to these organic Gd chelators, inorganic ligands receive little attention in the area.[8,9] The focus of this work is the fact that Gd–polyoxometalates (Gd–POMs) may be potential contrast agents for MRI, and the prospective employment of Gd–POMs in vivo in this context may turn out to be promising. The possible toxicity of a metal complex is related, in part, to its stability in vivo and its tissue clearance behavior. Even though testing and mechanistic understanding of complex toxicity requires the expertise of toxicologists and pharmacologists and syntheses by chemists, chelates with large formation constants and high stability in physiological environment remain a general

[a] Beijing National Laboratory for Molecular Science, Key Laboratory of Photochemistry, Institute of Chemistry, Chinese Academy of Science,
100190 Beijing, China
E-mail: jnyao@iccas.ac.cn
[b] Graduated School of Chinese Academy of Sciences,
100039 Beijing, China
[c] Key Laboratory of Green Process Engineering, Institute of Process Engineering, Chinese Academy of Science,
100190 Beijing, China
E-mail: zhanggj@home.ipe.ac.cn
[d] Jacobs University, School of Engineering and Science,
P. O. Box 750 561, 28725 Bremen, Germany
[e] Laboratoire de Chimie Physique, UMR 8000 CNRS, Université Paris-Sud 11,
91405 Orsay Cedex, France
E-mail: bineta.keita@lcp.u-psud.fr
[f] INSERM U759/Institut Curie-Recherche, Centre Universitaire Paris-Sud,
91405 Orsay Cedex, France
Supporting information for this article is available on the WWW under http://dx.doi.org/10.1002/ejic.200900610.

prerequisite for MRI usefulness. It fortunately happens that the few measured stability constants of lanthanide–POMs, including Gd–POMs, are high.[10–12] In addition, such values compare well with those of classical organic chelates already used in MRI assays: for example, $\log K$ = 17.4 for $[Gd(EDTA)(H_2O)_n]$[8] is very close to $\log K$ = 17.04 for $[Gd(\alpha_2\text{-}P_2W_{17}O_{61})_2]^{17-}$.[10] Finally, important complementary challenges will be to select (vide infra) a Gd–POM stable at physiological pH with a well-established structure. Recently, several monolanthanide-containing silicotungstates were synthesized, including the Gd-containing tungstosilicate $[Gd(\beta_2\text{-}SiW_{11}O_{39})_2]^{13-}$ (**1**).[13] The structure of this POM (Figure 1) shows that the Gd atom is sandwiched by two lacunary Keggin structures. Study on the biofunction of Gd–POMs is important for their further application as MRI agents. From our previous studies, HSA is an ideal model for the characterization of the biofunction of POMs. Complex **1**-HSA may also become a new MRI agent. In the current research, we studied the molecular interaction between Gd–POM and HSA.

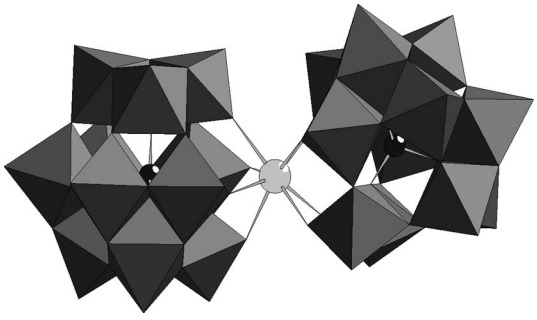

Figure 1. Combined polyhedral/ball-and-stick representation of $[Gd(\beta_2\text{-}SiW_{11}O_{39})_2]^{13-}$ (**1**). Color code: WO_6 grey octahedra, Si black, Gd light grey.

Results and Discussion

Prior to interaction studies, the stability of polyanion **1** in the pH 7.5 medium employed here was checked by UV/Vis spectrophotometry. The absorbances and peak wavelengths were monitored and found to be constant and reproducible over a period of several hours, largely exceeding the durations of POM–HSA interaction measurements.

The interaction between polyanion **1** and HSA was studied by fluorescence quenching. As we reported previously, the fluorescence of HSA, which is due to the single tryptophan residue in the protein Trp214 was efficiently quenched in the presence of POMs. Here we found that polyanion **1** can also quench the fluorescence of the protein efficiently. The variation of the HSA fluorescence spectrum upon addition of the POM is shown in Figure 2. A Stern–Volmer analysis was applied to the fluorescence quenching data. The Stern–Volmer plot of the fluorescence quenching in Figure 2b shows an upward curvature relationship. The upward characteristic of the plot indicates that there is not a purely static quenching mechanism. The quenching also showed strong ionic strength dependence: with the increase in the ionic strength of the solution, the quenching efficiency decreased significantly (Figure 2b). This means that strong static electrostatic interactions take place between polyanion **1** and HSA.

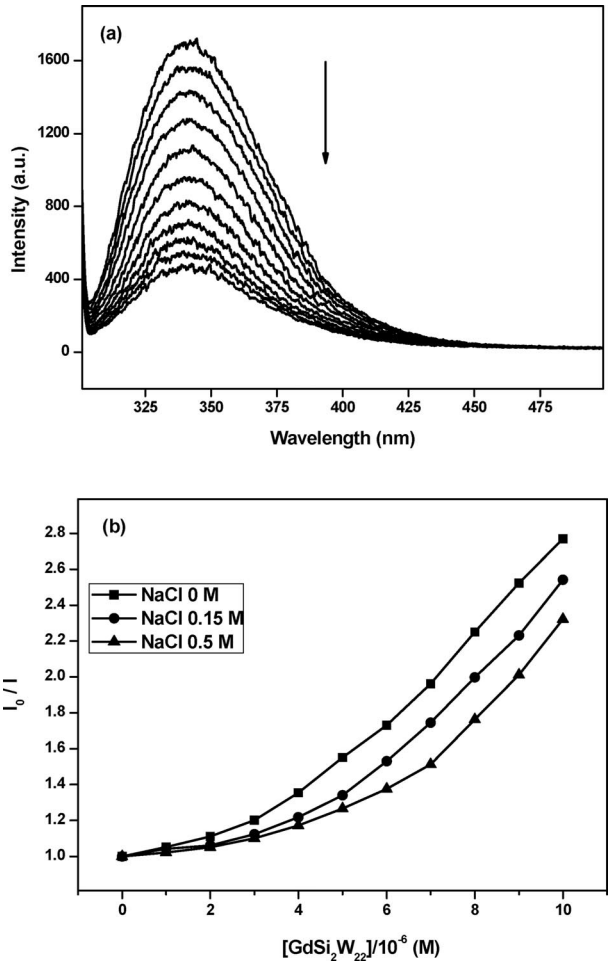

Figure 2. (a) Emission fluorescence spectra of HSA in the absence and in the presence of various concentrations of **1** ([HSA] = 1.0×10^{-5} M; from top to bottom, the concentration of **1** increased stepwise from 0 to 1.0×10^{-5} M with increments of 1.0×10^{-6} M); (b) Stern–Volmer plot of quenching of HSA fluorescence at different ionic strengths.

For further insight into the fluorescence quenching processes, the lifetime of the excited state of tryptophan within the protein was measured in the absence and in the presence of POMs. Figure 3 gives two typical decay curves of the fluorescence in the absence and in the presence of the POM, from which it can be directly seen that the lifetime decreased upon addition of **1**. The curves are correctly fitted and two typical lifetime values were obtained from the raw data. Table 1 gives the values of the fitted lifetime at different concentrations of **1**. In the absence of the polyanion, the lifetime falls within the estimations of lifetime for the single tryptophan of HSA.[4] It can be seen that both components of the lifetime decreased with increasing concentration of **1**. The decrease in the lifetime with polyanion addition indicates that energy transfer between **1** and the pro-

tein occurred. The mechanism also explained the upward shape of the Stern–Volmer plots of the fluorescence quenching, which can be attributed to energy-transfer-enhanced static quenching.

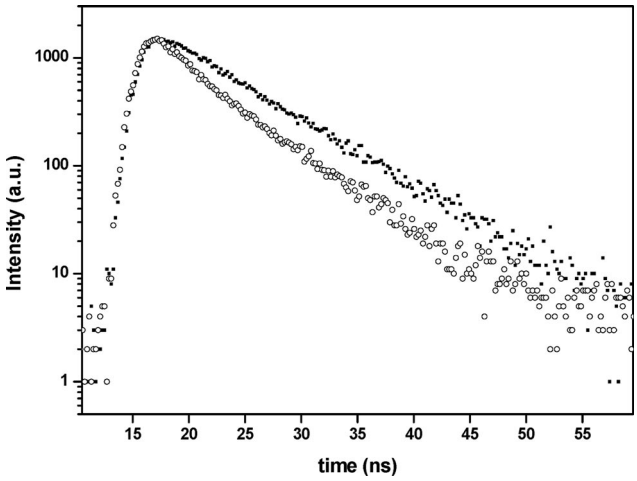

Figure 3. The fluorescence decay of HSA in the absence (filled circles) and the presence (open circles) of **1**. The protein was excited at 295 nm and monotored at 354 nm. The concentration of HSA was 1×10^{-5} M; the concentration of the POM in the trace with open circles was 1×10^{-5} M.

Table 1. Lifetimes of HSA (10 μM) at different concentrations of **1**.

	1/[HSA]					
	0	0.2	0.4	0.6	0.8	1.0
τ1 / ns	2.16	1.93	1.87	1.73	1.65	1.59
τ2 / ns	6.61	6.45	6.36	6.17	5.91	5.88

The interaction between **1** and HSA was further studied by CD spectroscopy to determine the effect of POM binding on the protein secondary structure. With an increase in the concentration of **1**, the CD signal decreased significantly (Figure 4). Such a decrease in the CD signal stopped when the molar ratio between **1** and the protein reached 1. Further addition of **1** did not have a significant effect on the CD signal, indicating that the polyanion formed a 1:1 complex with the protein.

Thermal denaturation experiments could also provide some information on such an interaction, as appears from Figure 5. In the absence of any ligand, HSA shows cooperative thermal unfolding in the 55–85 °C range, with a mid-temperature at approximately 65 °C. Binding of **1** has a remarkable effect on the thermal unfolding process of the protein. The thermal denaturation of the 1:1 complex of POM–HSA induced less unfolding of the protein, whereas the mid-temperature increases to over 70 °C.

To better understand the interaction between HSA and polyanion **1**, a complete characterization of the binding energetics was carried out by isothermal titration calorimetry (ITC) in an attempt to correlate the thermodynamic data with the results of other techniques.

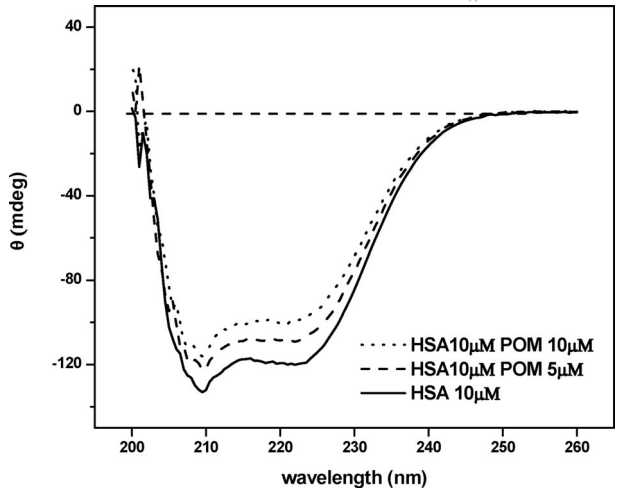

Figure 4. CD spectra of HSA in the absence and in the presence of different concentrations of **1** (in 10 mM Tris/HCl buffer, pH 7.5, 20 °C).

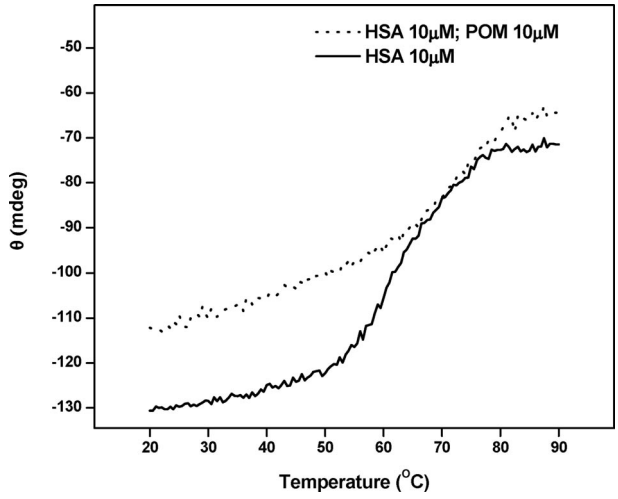

Figure 5. Thermal denaturation of the protein monitored by the CD signal at 222 nm in the absence and in the presence of **1**.

A representative calorimetric titration profile of 0.30 mM of **1** with 0.03 mM HSA at pH 7.5 and 30 °C is shown in Figure 6. $[Gd(\beta_2\text{-}SiW_{11}O_{39})_2]^{13-}$ shows a 1:1 binding stoichiometry to HSA with a binding constant of 3.3×10^6 M^{-1}, which indicates a strong and specific interaction. This is very close to the result obtained with a Keggin-type POM under the same experimental conditions (3×10^6 M^{-1}), with which a higher binding constant (1×10^7 M^{-1}) was measured at pH 3.5.[5] The binding is an exothermic process with a reaction enthalpy of –48.8 kJ mol^{-1}. The corresponding standard free energy of binding (ΔG) and the entropy contribution ($T\Delta S$) are –37.8 and – 11.0 kJ mol^{-1}, respectively. This means that the binding reaction is enthalpy driven, whereas the entropy component is unfavorable. The values of the thermodynamic parameters are very close to the reported data for the Keggin–HSA system.[4,5]

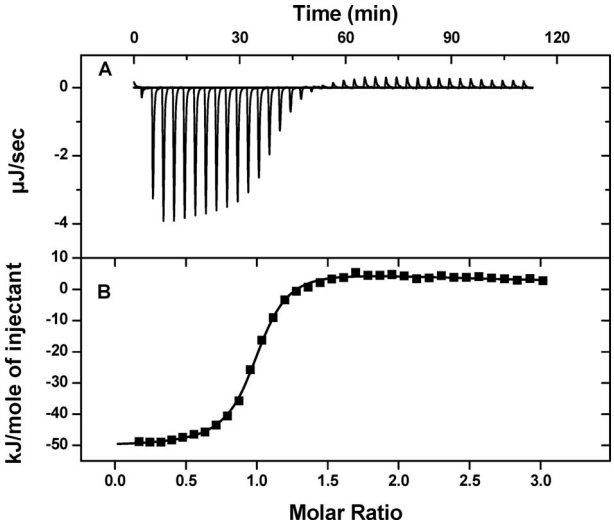

Figure 6. Thermogram and the isotherm corresponding to **1** binding to HSA. Aliquots of a solution of $Gd(\beta_2\text{-}SiW_{11}O_{39})_2$ (300 μM) were added to 30 μM HSA at 30 °C, in 50 mM Tris/HCl, pH 7.5. Each peak in panel A represents a single injection of the POM solution into the protein solution. Panel B shows the plot of the amount of heat liberated per mol of injectant as a function of the molar ratio of **1** to the protein. A standard best nonlinear least-square fit to a single binding site model is shown by the solid line.

Conclusions

In summary, the interaction between the Gd-containing tungstosilicate $[Gd(\beta_2\text{-}SiW_{11}O_{39})_2]^{13-}$ (**1**) and HSA was studied. The POM forms a 1:1 complex with HSA. The binding of **1** significantly alters the secondary structure of the protein. The simple stoichiometry observed in this work will open the way for complementary investigations including further design of novel Gd-containing inorganic components that could be used as novel agents in MRI imaging.

Experimental Section

Materials: Fatty-acid-free human serum albumin was purchased from Sigma. The samples were dissolved in a buffer solution (0.05 M Tris, pH 7.5). The concentration of the protein was determined spectrophotometrically by using an extinction coefficient of $\varepsilon_{280} = 36600\ M^{-1}\,cm^{-1}$. All chemicals were of high-purity grade and were used as purchased without further purification. Ultrapure water with a resistivity of 18.2 MΩcm was produced by passing through a RiOs 8 unit followed by a Millipore-Q Academic purification set. Polyanion **1** was synthesized following the reported procedure.[13]

UV/Vis Spectrophotometry: The stability of **1** in the pH 7.5 medium used here was assessed by UV/Vis spectroscopy with a Lambda 19 Perkin–Elmer spectrophotometer.

Fluorescence Methods: All fluorescence spectra were recorded with a FL4500 (Hitachi) fluorescence spectrophotometer. Quartz cuvettes with 1.0-cm optical path were used. The excitation wavelength was selected at 295 nm to avoid the excitation of tyrosine residues. The UV/Vis spectra were recorded at room temperature with a Perkin–Elmer Lambda 350 spectrophotometer. All the measurements were performed at room temperature (20 °C) in buffer solution, unless otherwise stated. Typically, 2 mL of a solution containing an appropriate concentration of HSA was titrated by successive additions of aliquots of POM solutions. Titrations were performed manually by using syringes. At each addition, the fluorescence spectrum was collected. Raw data were systematically corrected for inner filter effects. Time-resolved fluorescence lifetimes were obtained from the fluorescence decays by using time-correlated single photon counting technique by Edinburgh Analytical Instruments – FLS920.

Circular Dichroism (CD) Spectroscopy: CD experiments were performed with a Jasco 715 spectropolarimeter equipped with a Peltier temperature control unit. Far-UV spectra were recorded between 200 and 260 nm at 20 °C by using 1-mm quartz cells. Samples were dissolved in 10 mM Tris buffer (pH 7.5). Temperature denaturation curves were recorded between 20 and 90 °C with a temperature increase rate of $1\ °C\,min^{-1}$.

Isothermal Titration Calorimetry (ITC): ITC experiments were performed by using a MicroCal MCS instrument (MicroCal Inc., Northampton, MA). Protein and POM solutions were properly degassed prior to the titrations to avoid the formation of bubbles in the calorimeter cell. The protein (10–30 μM) in the 1.337 mL calorimeter cell was titrated by the POM solution (generally 10–30 times more concentrated) by successive automatic injections of 8 μL each. The first injection of 2 μL was ignored in the final data analysis. Integration of peaks corresponding to each injection and correction for the baseline were carried out by using Origin-based software provided by the manufacturer. Fitting the data to various interaction models results in the stoichiometry (n), equilibrium binding constant (K_a), and enthalpy of complex formation (ΔH). The other thermodynamic parameters were calculated according to the formulae given in Equations (1) and (2).

$$\Delta G = \Delta H - T\Delta S \quad (1)$$

$$\Delta G = -RT\ln K_a \quad (2)$$

where T is the absolute temperature (in the current experiment T = 303 K) and $R = 8.3151\ J\,mol^{-1}\,K^{-1}$.

Supporting Information (see footnote on the first page of this article): Synthesis of polyanion **1**.

Acknowledgments

This work was supported by the Marie Curie International Incoming Fellowship from the European Community (contract No. 040487), the One Hundred Talent Program of the Chinese Academy of Science, the National Natural Science Foundation of China (No. 20733006, 50720145202), the National Basic Research Program of China (No. 2006CB806200), Jacobs University, the German Science Foundation (DFG) (KO-2288/8–1), the Fonds der Chemischen Industrie, the Centre National de la Recherche Scientifique (CNRS) (UMR 8000), the Université Paris-Sud 11, France, and the INSERM U 759/Institut Curie–Recherche.

[1] a) M. T. Pope, *Heteropoly and Isopoly Oxometalates*, Springer, New York, **1983**; b) M. T. Pope, A. Müller, *Angew. Chem. Int. Ed. Engl.* **1991**, *30*, 34–48.
[2] B. Keita, L. Nadjo, "Electrochemistry of Isopoly and Heteropoly Oxometalates" in *Encyclopedia of Electrochemistry* (Eds.: A. J. Bard, M. Stratmann, F. Scholz, C. J. Pickett), Wiley, New York, **2006**, vol. 7, pp. 607–700.
[3] a) D. A. Judd, J. H. Nettles, N. N. Nevins, J. P. Snyder, D. C. Liotta, J. Tang, J. Ermolieff, R. F. Schinazi, C. L. Hill, *J. Am.*

Chem. Soc. **2001**, *123*, 886–897; b) J. T. Rhule, C. L. Hill, D. A. Judd, R. F. Schinazi, *Chem. Rev.* **1998**, *98*, 327–358; c) T. Yamase, *J. Mater. Chem.* **2005**, *15*, 4773–4782.

[4] G. Zhang, B. Keita, J. C. Brochon, P. Oliveira, L. Nadjo, C. T. Craescu, S. Miron, *J. Phys. Chem. B* **2007**, *111*, 1809–1814.

[5] G. Zhang, B. Keita, C. T. Craescu, S. Miron, P. Oliveira, L. Nadjo, *J. Phys. Chem. B* **2007**, *111*, 11253–11259.

[6] G. Zhang, B. Keita, C. T. Craescu, S. Miron, P. Oliveira, L. Nadjo, *Biomacromolecules* **2008**, *9*, 812–817.

[7] G. Hungerford, K. Suhling, M. Green, *Photochem. Photobiol. Sci.* **2008**, *7*, 734–737.

[8] R. B. Lauffer, *Chem. Rev.* **1987**, *87*, 901–927.

[9] S. Aime, A. Barge, C. Cabella, S. G. Crich, E. Gianolio, *Curr. Pharm. Biotechnol.* **2004**, *5*, 509–518.

[10] Y.-W. Lu, B. Keita, L. Nadjo, *Polyhedron* **2004**, *23*, 1579–1586 and references cited therein.

[11] C. Zhang, L. Bensaid, D. McGregor, X. Fang, R. C. Howell, B. Burton-Pye, Q. Luo, L. Todaro, L. C. Francesconi, *J. Cluster Sci.* **2006**, *17*, 389–425.

[12] J.-P. Ciabrini, R. Contant, *J. Chem. Res. (M)* **1993**, 2720–2744; J.-P. Ciabrini, R. Contant, *J. Chem. Res. (S)* **1993**, 391.

[13] B. S. Bassil, M. H. Dickman, B. von der Kammer, U. Kortz, *Inorg. Chem.* **2007**, *46*, 2452–2458.

Received: June 30, 2009
Published Online: October 7, 2009

